629.13 09
N11n 39
GOVT. DOC.
Y3.N21/5 :6/2007

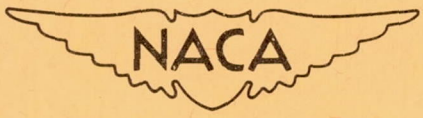
NATIONAL ADVISORY COMMITTEE FOR AERONAUTICS

TECHNICAL NOTE 2007

THE LOAD DISTRIBUTION DUE TO SIDESLIP ON TRIANGULAR, TRAPEZOIDAL, AND RELATED PLAN FORMS IN SUPERSONIC FLOW

By Arthur L. Jones and Alberta Alksne

Ames Aeronautical Laboratory
Moffett Field, Calif.



Washington
January 1950

COUNTY STATE LIBRARY

JAN 13 1950

BUSINESS, SCIENCE
& TECHNOLOGY DEP'T.

NATIONAL ADVISORY COMMITTEE FOR AERONAUTICS

TECHNICAL NOTE 2007

THE LOAD DISTRIBUTION DUE TO SIDESLIP ON TRIANGULAR, TRAPEZOIDAL, AND RELATED PLAN FORMS IN SUPERSONIC FLOW

By Arthur L. Jones and Alberta Alksne

SUMMARY

Expressions are presented for the load distribution on a representative group of plan forms in sideslip at supersonic speeds. These expressions were obtained by the application of lifting-surface theories based on the linearized equation for compressible flow. Sketches of the load distributions are included.

INTRODUCTION

In three recent reports (references 1, 2, and 3) the variations of rolling moment, of yawing moment, and of lift and pitching moment with sideslip have been investigated for a group of wing plan forms for supersonic speeds. The pressure distributions required to compute these forces and moments were calculated using linearized compressible-flow theory for thin airfoils. Since the reports referred to were concerned with the detailed expressions of moments and forces for the various plan forms, it was decided that the reference value of the pressure distributions, their possible utility in stress analysis and design, and the desirability of including some pictorial representations justified the treatment of these distributions as the subject of a separate report.

By virtue of the many approximations involved in its derivation, the linearized theory applied constitutes one of the most simplified analytical approaches to compressible-flow problems. Furthermore, in addition to the factors approximated in the linearization of the potential theory, the analysis employed does not account for the lack of complete rigidity of a wing nor the effects of viscosity in the flow. These are two important factors that may have considerable effect on the actual distribution of the pressure on a wing. Thus, it is not expected that these pressure distributions will conform precisely to those obtained in the actual physical flow. It is expected, however, that these theoretical solutions will be good first approximations for the plan forms and conditions considered herein and they should provide satisfactory indications of the pressure-difference contours in general if not in detail.

The investigation covers the following configurations: (See figs. 1 and 2.) (1) Triangular plan forms with subsonic leading edges or with supersonic leading edges; (2) trapezoidal plan forms with all possible combinations of raked-in, raked-out, subsonic, or supersonic tips; (3) rectangular plan forms; and (4) two swept-back plan forms with supersonic trailing edges developed from the triangular wings. Illustrations are included in order to provide a convenient visual correlation between the expressions for the pressure distributions and for the moments and forces that were calculated from them (references 1, 2, and 3). The arrangement of the appendixes was based on the desire to present a systematic and convenient compilation of expressions and illustrations for the load distributions for the various plan forms considered.

SYMBOLS, COEFFICIENTS, AND AXES

A aspect ratio $\left(\frac{b^2}{S}\right)$

b span of wing measured normal to plane of symmetry

B Mach number parameter $\left(\sqrt{M_1{}^2-1}\right)$

Bm ratio of tangent of right tip angle to tangent of Mach cone angle $\left(\frac{m}{\tan \mu}\right)$

c_r chord of wing in plane of symmetry

$E(\varphi,k)$ incomplete elliptic integral of the second kind with modulus k $\left(\int_0^{\varphi} \sqrt{1-k^2 \sin^2 \theta}\, d\theta\right)$

E complete elliptic integral of the second kind with modulus k $\left[E\left(\frac{\pi}{2},k\right)\right]$

$F(\varphi,k)$ incomplete elliptic integral of the first kind with modulus k $\left(\int_0^{\varphi} \frac{d\theta}{\sqrt{1-k^2 \sin^2 \theta}}\right)$

K complete elliptic integral of the first kind with modulus k $\left[F\left(\frac{\pi}{2},k\right)\right]$

l over-all longitudinal length of swept-back wing

m slope of right wing tip measured in plane of wing (positive for raked-out tip, negative for raked-in tip)

M_1	free-stream Mach number
n_0, n_1	slopes of plan-form edges relative to wind axes
ΔP	pressure differential across wing surface, positive upward
$\frac{\Delta P}{q}$	loading coefficient
q	free-stream dynamic pressure $\left(\frac{\rho}{2} V^2\right)$
S	area of wing
u	perturbation velocity parallel to positive x axis
V	free-stream velocity
w	perturbation velocity parallel to z axis (positive upward)
x,y,z	rectangular coordinates of wind axes (fig. 3)
α	angle of attack, radians
β	sideslip angle (positive when sideslipping to right), degrees
μ	Mach angle $\left(\tan^{-1} \frac{1}{B}\right)$
ξ,η,ζ	rectangular coordinates of stability axes (fig. 3)
ξ',η',ζ'	rectangular coordinates of body axes (fig. 3)
ρ	air density in the free stream
φ	perturbation velocity potential

Subscripts

$A,B,\ldots V$	expressions given in Appendix B

The body axes are generally a right-handed system of three orthogonal axes as shown in figure 3 with the longitudinal axis ξ' lying in the plane of the wing. The stability axes are, in effect, the body axes rotated about the lateral axis η' (through $-\alpha$) until the longitudinal axis is in the horizontal plane containing the free-stream vector; a subsequent rotation about the vertical axis ζ (through β) would bring the longitudinal axis in line with the free-stream vector and the axes would now be coincident with the wind axes.

It should be mentioned that the orientation of these axes as shown in figure 3 is convenient for the calculations required to determine the pressure distributions and the resulting forces and moments. In the application of these results to the calculation of the motion and dynamic stability of an airplane, however, the axes are usually rotated so that the positive direction of the longitudinal axis is into the free stream and the positive direction of the vertical axis is downward, that is, toward the undercarriage of the airplane.

METHOD OF ANALYSIS

The development of the expressions for the pressure (i.e., load) distributions on wing plan forms in sideslip was merely an application of supersonic wing theory. In this report, only the part of the theory relating to the flat-plate or so-called "additional" loading, which is the loading resulting from a change in angle of attack, will be considered. The loadings due to camber and twist are usually assessed independently, and the sum of these two loadings is often referred to as the "basic" load distribution.

By linearization of the partial differential equation for compressible flow it is possible to develop a simplified lifting-surface theory for thin airfoils. The linearization is made possible by the assumption that, for thin airfoils, the perturbation velocities induced by the airfoil are small relative to the free-stream velocity. If the free-stream velocity vector is parallel to and in the direction of the positive x axis and if φ denotes the perturbation velocity potential for isentropic flow, the linearized partial differential equation for steady-state conditions at supersonic velocities is

$$\left(M_1^2-1\right)\frac{\partial^2\varphi}{\partial x^2}-\frac{\partial^2\varphi}{\partial y^2}-\frac{\partial^2\varphi}{\partial z^2}=0$$

where M_1 is the Mach number of the free stream. There have been a number of methods developed that provide means of fitting solutions of this equation to the boundary conditions of thin-airfoil theory (e.g., references 4 through 9). The results to be given herein were determined through the general use of source-sink and doublet distributions (references 4, 5, 6, and 9). In particular, the method of reference 6 was applied to cases where a subsonic tip occurs in conjunction with a supersonic leading edge or tip; whereas the load distributions for all other edge and Mach cone arrangements were calculated by application of the methods summarized in reference 9.

The first step in the analysis is the establishment of the boundary conditions. For thin airfoils the boundary conditions are usually restricted to the $z=0$ plane. Thus, if the local angles of attack at various spanwise stations of the wing are specified and it is assumed

that the wing is coincident with the $z=0$ plane, the boundary conditions are set. Next, the expressions for the loading $\frac{\Delta P}{q}$ and the angle of attack α are formulated in terms of parameters that can be related to the potential solutions of the differential equation and to the boundary conditions. For linearized theory these relationships are

$$\frac{\Delta P}{q} = \frac{4u}{V} \text{ (if } u \text{ is for the upper surface)}$$

where

$$u = \frac{\partial \varphi}{\partial x}\Big]_{z=0}$$

and

$$\alpha = -\frac{w}{V}$$

where

$$w = \frac{\partial \varphi}{\partial z}\Big]_{z=0}$$

Thus the problem is reduced to determining φ in such a manner that $-\frac{w}{V}$ is equal to the specified local angle of attack at every spanwise station of the wing.

The general problem of specifying the angle of attack and of solving for the resulting velocity potential is one that usually requires the solution of an integral equation. (See reference 9.) For cases where the edges of the plan form are supersonic, however, the lack of interaction between the upper and lower surfaces of the wing permits the problem to be solved by a distribution of sources in accordance with the local slopes of the plan form and a straightforward integration of their potentials. The triangular and trapezoidal plan forms with supersonic edges were treated in this manner. Likewise, wherever a subsonic edge is in conjunction with a supersonic leading edge or tip a straightforward integration can be employed. For this case reference 6 provides a method, based on the consideration of the upwash between the subsonic edge and the Mach cone, whereby the usual operations involved in the solution of the integral equation are eliminated. In general, however, it is necessary to go through rather involved procedures to calculate the load distribution when the camber, twist, and angle of attack of the plan form are specified. These procedures are discussed in reference 9 wherein, for conical-flow conditions, a loading element is used to set up the integral equation and then the usual integral-equation techniques are employed to solve it.

It should be mentioned also that, when the trailing edge is subsonic, an additional stipulation based on some physical concept for the

flow, such as the Kutta condition which is applied herein, is needed in order to eliminate all but one of an infinite number of potential solutions that will satisfy the boundary conditions.

PRESENTATION OF RESULTS

All the plan forms and conditions investigated in references 1, 2, and 3 were made up using the five following combinations of straight edges:

1. A supersonic leading edge in conjunction with a subsonic leading edge

2. A supersonic leading edge in conjunction with a subsonic trailing edge

3. Two subsonic leading edges

4. A subsonic leading edge in conjunction with a subsonic trailing edge

5. Two supersonic leading edges

The expressions for the load distributions on these five combinations are given in Appendix A in terms of the wind-axes notation.

In order to provide an easy correlation between the load distributions and the aerodynamic characteristics of the plan forms presented in references 1, 2, and 3, Appendix B contains the expressions for the load distributions on various sectors of the plan forms in terms of the plan-form parameters and the body-axes notation. Since the plan forms are restricted to the $z=0$ plane for the purpose of analysis by the thin-airfoil theory, the body-axes notation, in a sense, refers to coordinates on the projection of the plan form onto the $z=0$ plane, which corresponds to giving the coordinates in terms of the stability-axes notation. This slight ambiguity between the body axes and the stability axes, caused by the assumptions employed in thin-airfoil theory, should not be allowed to cause any doubt about the direction of the normal force. This force acts perpendicular to the plate and in a direction parallel to the ζ' axis, not the ζ axis.

The order of presentation of the plan-form sectors in Appendix B of this report is a duplicate of the arrangements of the Appendixes B of references 1, 2, and 3. A sketch of the load distribution is presented for each sector in Appendix B in order to provide a convenient visual interpretation of the load distribution.

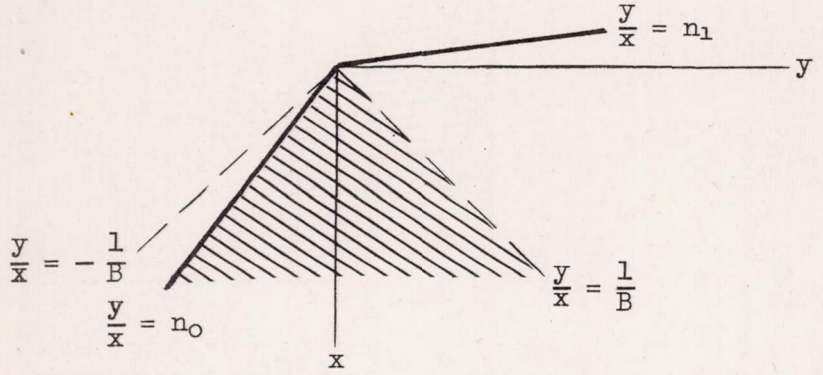
Ames Aeronautical Laboratory,
National Advisory Committee for Aeronautics,
Moffett Field, Calif., Oct. 10, 1949.

APPENDIX A

SUMMARY OF EXPRESSIONS FOR LOAD DISTRIBUTION ON WING ELEMENTS IN TERMS OF WIND-AXES NOTATION

Expressions Apply to Crosshatched Plan-Form Areas

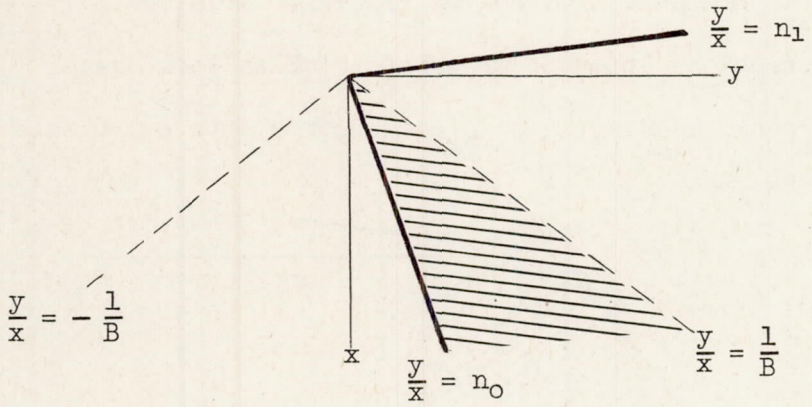
1. Supersonic leading edge in conjunction with a subsonic leading edge:



$$\frac{\Delta P}{q} = \frac{4\alpha}{\pi B}\left[\frac{2\sqrt{1-\frac{n_o}{n_1}}}{\left(1-\frac{1}{Bn_o}\right)\sqrt{1+\frac{1}{Bn_1}}}\sqrt{\frac{1-\frac{By}{x}}{\frac{By}{x}-Bn_o}}+\right.$$

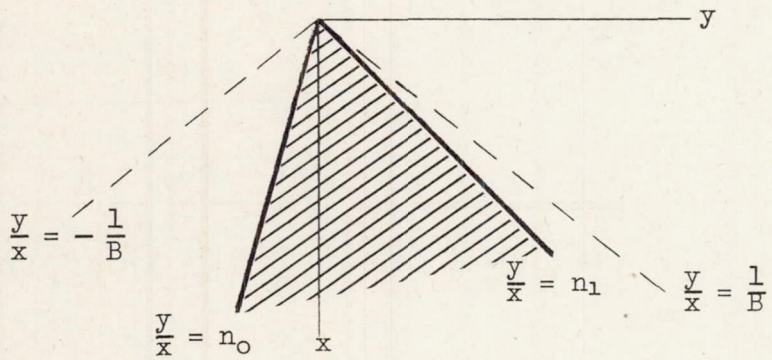
$$\left.\frac{2}{\sqrt{1-\left(\frac{1}{Bn_1}\right)^2}}\tan^{-1}\sqrt{\frac{\left(1-\frac{1}{Bn_1}\right)\left(\frac{By}{x}-Bn_o\right)}{\left(1-\frac{n_o}{n_1}\right)\left(1-\frac{By}{x}\right)}}\right]$$

2. Supersonic leading edge in conjunction with a subsonic trailing edge:



$$\frac{\Delta P}{q} = \frac{8\alpha}{\pi B \sqrt{1-\left(\frac{1}{Bn_1}\right)^2}} \tan^{-1} \sqrt{\frac{\left(1-\frac{1}{Bn_1}\right)\left(\frac{By}{x} - Bn_o\right)}{\left(1-\frac{n_o}{n_1}\right)\left(1-\frac{By}{x}\right)}}$$

3 Two subsonic leading edges:



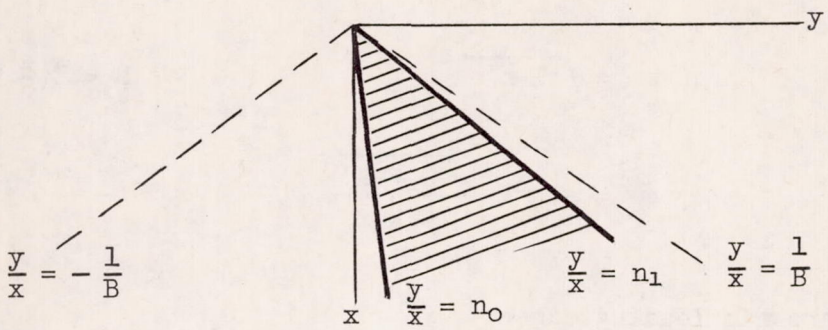
$$\frac{\Delta P}{q} = \frac{2\alpha}{E} \sqrt{\frac{2G}{B(n_1-n_o)}} \left[\frac{(n_1+n_o)\frac{y}{x} - 2n_1n_o}{\sqrt{\left(-n_o+\frac{y}{x}\right)\left(n_1-\frac{y}{x}\right)}} \right]$$

where

E is the complete elliptic integral of the second kind with modulus $\sqrt{1-G^2}$

$$G = \frac{1-B^2 n_1 n_o - \sqrt{(1-B^2 n_1^2)(1-B^2 n_o^2)}}{B(n_1-n_o)}$$

4. Subsonic leading edge in conjunction with a subsonic trailing edge:



$$\frac{\Delta P}{q} = \frac{4\alpha}{B} P \sqrt{\frac{\frac{y}{x} - n_o}{n_1 - \frac{y}{x}}}$$

when $n_o = 0$

$$P = \frac{1}{E\sqrt{2}} \sqrt{1-\sqrt{1-B^2 n_1^2}}$$

when $n_1 = \frac{1}{B}$

$$P = \frac{1}{\pi} \sqrt{\frac{2}{1-Bn_o}}$$

when $n_o > 0$; $n_1 < \frac{1}{B}$

$$P = \sqrt{\frac{Bn_1 - G_1}{(G_1-Bn_o)(1-G_1^2)}} \left\{ \frac{G_1 + k'}{\frac{k'K}{G_1} + E + \frac{k'\sqrt{1-G_1^2}}{\sqrt{G_1^2-k'^2}} \left[E\,F(\varphi,k) - K\,E(\varphi,k) \right]} \right\}$$

where

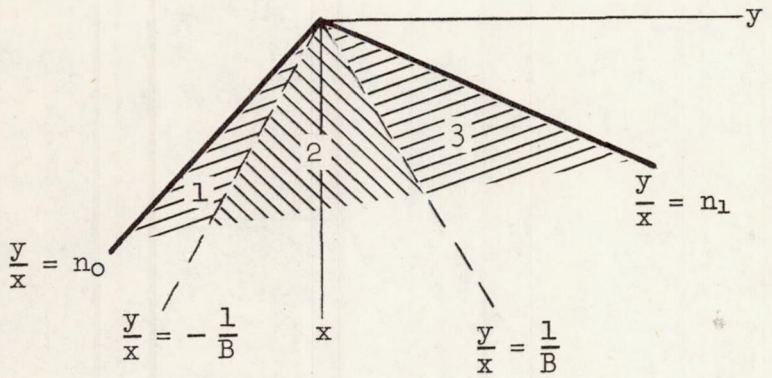
$$G_1 = \frac{1+B^2 n_1 n_o - \sqrt{(1-B^2 {n_1}^2)(1-B^2 {n_o}^2)}}{B(n_1+n_o)}$$

$$k' = \frac{G_1 - Bn_o}{1-BG_1 n_o} \qquad K = F\left(\frac{\pi}{2}, k\right)$$

$$k = \sqrt{1-k'^2} \qquad E = E\left(\frac{\pi}{2}, k\right)$$

$$\varphi = \sin^{-1} \frac{\sqrt{{G_1}^2 - k'^2}}{G_1 k}$$

5. Two supersonic leading edges:



$$\left(\frac{\Delta P}{q}\right)_1 = \frac{4\alpha}{\sqrt{B^2 - \frac{1}{{n_o}^2}}}$$

$$\left(\frac{\Delta P}{q}\right)_3 = \frac{4\alpha}{\sqrt{B^2 - \frac{1}{{n_1}^2}}}$$

$$\left(\frac{\Delta P}{q}\right)_2 = \frac{2\alpha}{\sqrt{B^2-\frac{1}{n_1^2}}} + \frac{4\alpha}{\pi\sqrt{B^2-\frac{1}{n_1^2}}} \sin^{-1}\left[\frac{n_1B^2\,\frac{y}{x}-1}{B\left(n_1-\frac{y}{x}\right)}\right] +$$

$$\frac{2\alpha}{\sqrt{B-\frac{1}{n_o^2}}} - \frac{4\alpha}{\pi\sqrt{B^2-\frac{1}{n_o^2}}} \sin^{-1}\left[\frac{-n_oB^2\,\frac{y}{x}+1}{B\left(-n_o+\frac{y}{x}\right)}\right]$$

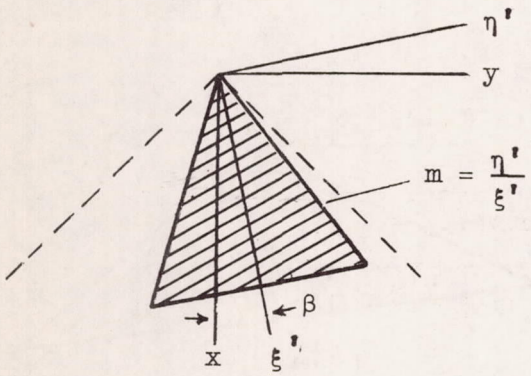
APPENDIX B

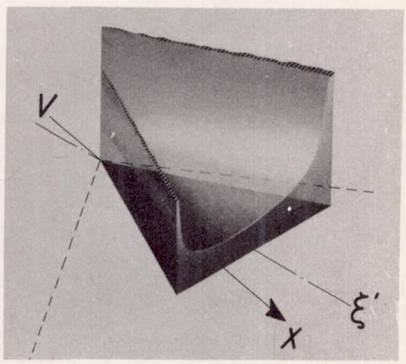
SUMMARY OF EXPRESSIONS FOR LOAD DISTRIBUTION IN TERMS OF BODY-AXES NOTATION

Expressions apply to crosshatched and heavily shaded plan-form areas

1. Triangular Wings:

A.





$$\left(\frac{\Delta P}{q}\right)_A = \frac{4\alpha}{E}\sqrt{\frac{G}{Bm(1+\tan^2\beta)}}\left[\frac{m^2+\frac{\eta'}{\xi'}\tan\beta}{\sqrt{\left(m+\frac{\eta'}{\xi'}\right)\left(m-\frac{\eta'}{\xi'}\right)}}\right]$$

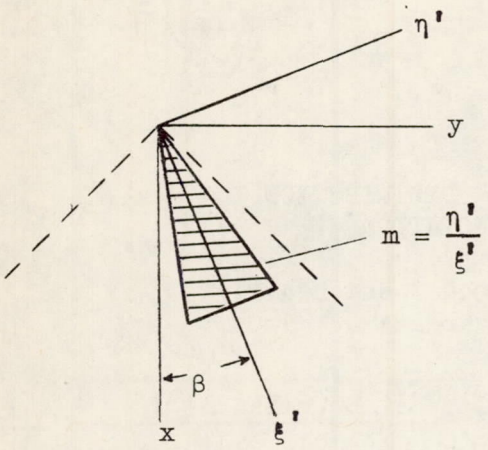
where

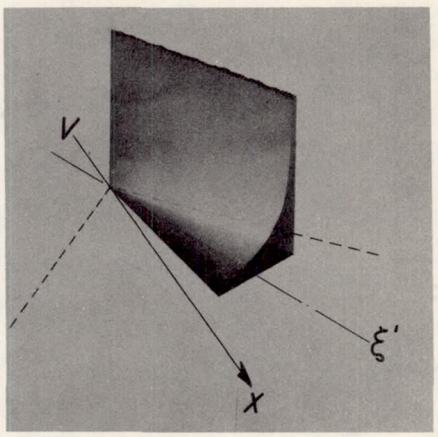
E is the complete elliptic integral of the second kind with modulus

$\sqrt{1-G^2}$

$$G = \frac{(1-m^2\tan^2\beta) + B^2(m^2-\tan^2\beta)}{2Bm(1+\tan^2\beta)} - \frac{\sqrt{[(1-m\tan\beta)^2-B^2(m+\tan\beta)^2][(1+m\tan\beta)^2-B^2(m-\tan\beta)^2]}}{2Bm(1+\tan^2\beta)}$$

B.





$$\left(\frac{\Delta P}{q}\right)_B = \frac{4\alpha P_1}{B}\sqrt{\frac{(m+\frac{\eta'}{\xi'})(1-m\tan\beta)}{(m-\frac{\eta'}{\xi'})(1+m\tan\beta)}}$$

when $\tan\beta = m$

$$P_1 = \frac{1}{E}\sqrt{\frac{G_1 Bm}{(1-m^2)}}$$

when $\tan\beta = \frac{1-Bm}{B+m}$

$$P_1 = \frac{\sqrt{2}\sqrt{1+m\tan\beta}}{\pi\sqrt{(1+m\tan\beta)+B(m-\tan\beta)}}$$

when $m < \tan\beta < \dfrac{1-Bm}{B+m}$

$$P_1 = \sqrt{\frac{[B(m+\tan\beta)-G_1(1-m\tan\beta)](1+m\tan\beta)}{[B(m-\tan\beta)+G_1(1+m\tan\beta)](1-m\tan\beta)(1-G_1^2)}}$$

$$\left\{ \frac{G_1+k'}{\dfrac{k'K}{G_1} + E + \dfrac{k'\sqrt{1-G_1^2}}{\sqrt{G_1^2-k'^2}}} \right.$$

$$\left. [E\,F(\varphi,k)-K\,E(\varphi,k)] \right\}$$

where

$$G_1 = \frac{(1-m^2\tan^2\beta)-B^2(m^2-\tan^2\beta)}{2B(1+m^2)\tan\beta} -$$

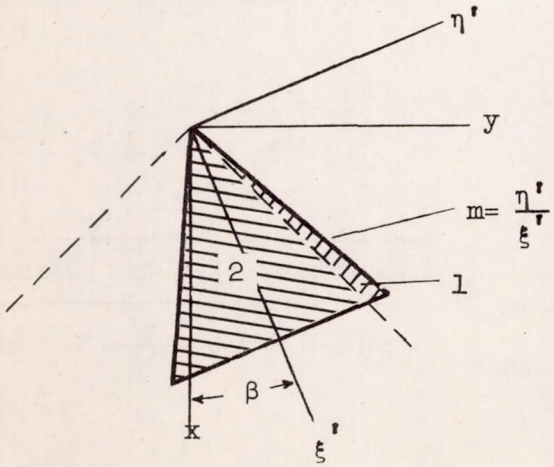
$$\frac{\sqrt{[(1+m\tan\beta)^2-B^2(m-\tan\beta)^2][(1-m\tan\beta)^2-B^2(m+\tan\beta)^2]}}{2B(1+m^2)\tan\beta}$$

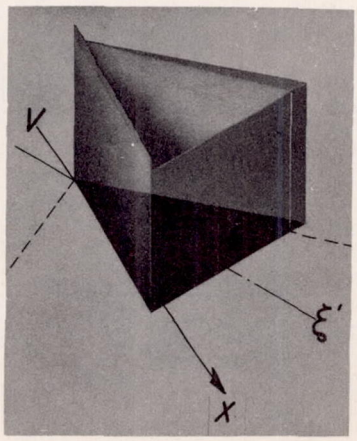
$$k = \sqrt{1-k'^2} \qquad k' = \frac{G_1(1+m\tan\beta)+B(m-\tan\beta)}{(1+m\tan\beta)+G_1B(m-\tan\beta)}$$

$$\varphi = \sin^{-1}\frac{G_1^2-k'^2}{G_1k}$$

$$K = F\left(\frac{\pi}{2},k\right);\quad E = E\left(\frac{\pi}{2},k\right)$$

C.





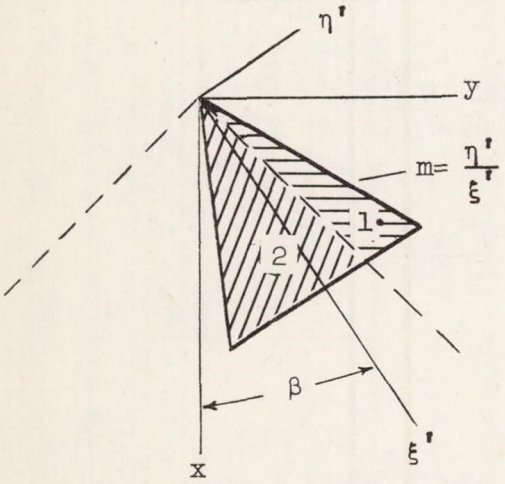
$$\left(\frac{\Delta P}{q}\right)_{C_1} = \frac{4\alpha(m+\tan\beta)}{\sqrt{B^2(m+\tan\beta)^2-(1-m\tan\beta)^2}}$$

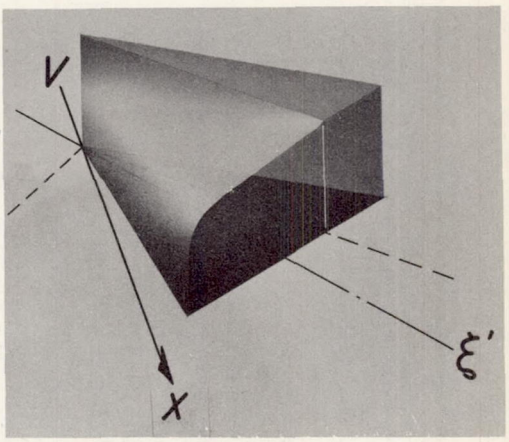
$$\left(\frac{\Delta P}{q}\right)_{C_2} = \frac{8\alpha(m+\tan\beta)}{\pi\sqrt{B^2(m+\tan\beta)^2-(1-m\tan\beta)^2}} \left\{ \frac{[B(m+\tan\beta)-(1-m\tan\beta)](m-\tan\beta)}{[B(m-\tan\beta)+(1+m\tan\beta)](m+\tan\beta)} \right.$$

$$\sqrt{\frac{2m[(1-B\tan\beta)-\frac{\eta'}{\xi'}(B+\tan\beta)]}{[m(B+\tan\beta)-(1-B\tan\beta)](m+\frac{\eta'}{\xi'})}} +$$

$$\left. \tan^{-1}\sqrt{\frac{[m(B+\tan\beta)-(1-B\tan\beta)](m+\frac{\eta'}{\xi'})}{2m[(1-B\tan\beta)-\frac{\eta'}{\xi'}(B+\tan\beta)]}} \right\}$$

D.

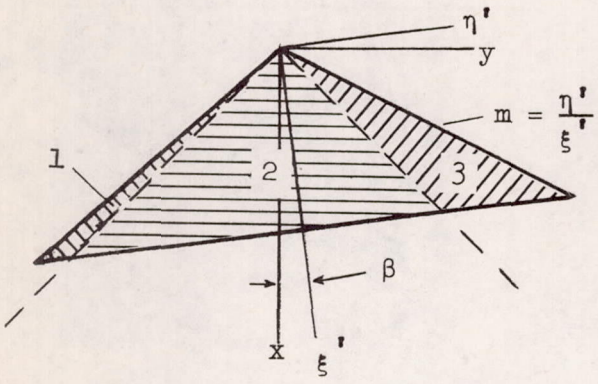


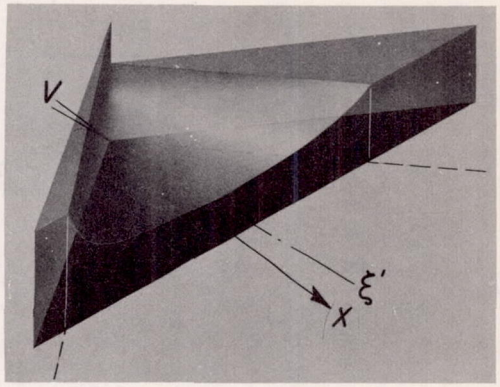


$$\left(\frac{\Delta P}{q}\right)_{D_1} = \frac{4\alpha(m+\tan\beta)}{\sqrt{B^2(m+\tan\beta)^2-(1-m\tan\beta)^2}}$$

$$\left(\frac{\Delta P}{q}\right)_{D_2} = \frac{8\alpha(m+\tan\beta)}{\pi\sqrt{B^2(m+\tan\beta)^2-(1-m\tan\beta)^2}} \tan^{-1}\sqrt{\frac{[m(B+\tan\beta)-(1-B\tan\beta)](m+\frac{\eta'}{\xi'})}{2m[(1-B\tan\beta)-\frac{\eta'}{\xi'}(B+\tan\beta)]}}$$

E. $\tan\beta < \frac{Bm-1}{B+m}$





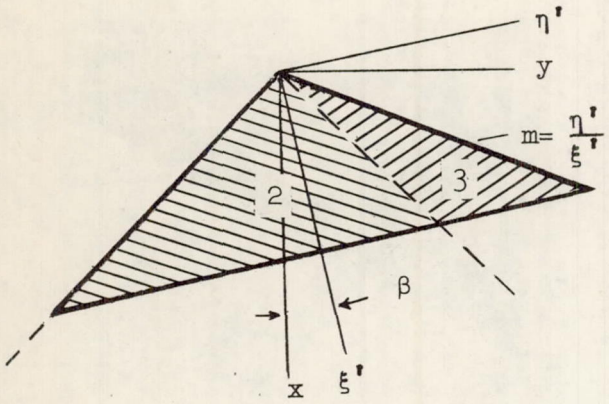
$$\left(\frac{\Delta P}{q}\right)_{E_1} = \frac{4\alpha(m-\tan\beta)}{\sqrt{B^2(m-\tan\beta)^2-(1+m\tan\beta)^2}}$$

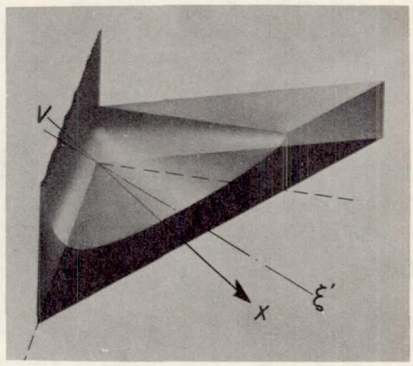
$$\left(\frac{\Delta P}{q}\right)_{E_2} = \frac{4\alpha(m+\tan\beta)}{\pi\sqrt{B^2(m+\tan\beta)^2-(1-m\tan\beta)^2}}\left[\frac{\pi}{2} + \sin^{-1}\frac{B^2(m+\tan\beta)\left(\frac{\eta'}{\xi'}+\tan\beta\right)-(1-m\tan\beta)\left(1-\frac{\eta'}{\xi'}\tan\beta\right)}{B\left(m-\frac{\eta'}{\xi'}\right)(1+\tan^2\beta)}\right] +$$

$$\frac{4\alpha(m-\tan\beta)}{\pi\sqrt{B^2(m-\tan\beta)^2-(1+m\tan\beta)^2}}\left[\frac{\pi}{2} - \sin^{-1}\frac{B^2(m-\tan\beta)\left(\frac{\eta'}{\xi'}+\tan\beta\right)+(1+m\tan\beta)\left(1-\frac{\eta'}{\xi'}\tan\beta\right)}{B\left(m+\frac{\eta'}{\xi'}\right)(1+\tan^2\beta)}\right]$$

$$\left(\frac{\Delta P}{q}\right)_{E_3} = \frac{4\alpha(m+\tan\beta)}{\sqrt{B^2(m+\tan\beta)^2-(1-m\tan\beta)^2}}$$

E*. $\tan \beta = \frac{mB-1}{B+m}$ (See footnote a.)





$$\left(\frac{\Delta P}{q}\right)_{E_2^*} = \frac{4\alpha(m^2+2mB-1)}{\pi\sqrt{B^2(m^2+2mB-1)^2-(B+2m-m^2B)}}\left\{\frac{\pi}{2} + \right.$$

$$\left. \sin^{-1}\frac{B^2(m^2+2mB-1)\left[(mB-1)+\frac{\eta'}{\xi'}(B+m)\right]-(B+2m-m^2B)\left[(B+m)-\frac{\eta'}{\xi'}(Bm-1)\right]}{B\left(m-\frac{\eta'}{\xi'}\right)\left[(B+m)^2+(mB-1)^2\right]}\right\} +$$

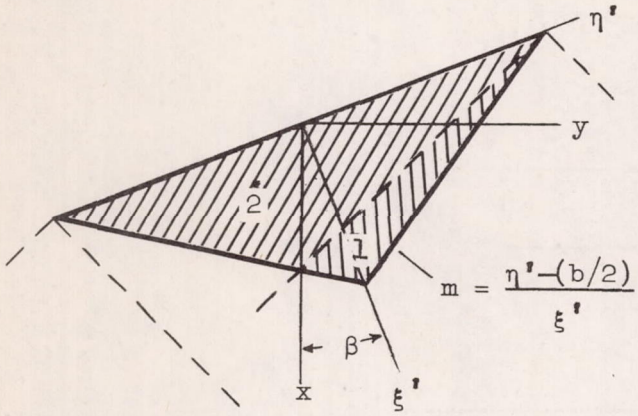
$$\frac{4\alpha}{\pi}\sqrt{\frac{(m+2B-B^2m)-\frac{\eta'}{\xi'}(B^2+2mB-1)}{(B^2+1)\left(m+\frac{\eta'}{\xi'}\right)}}$$

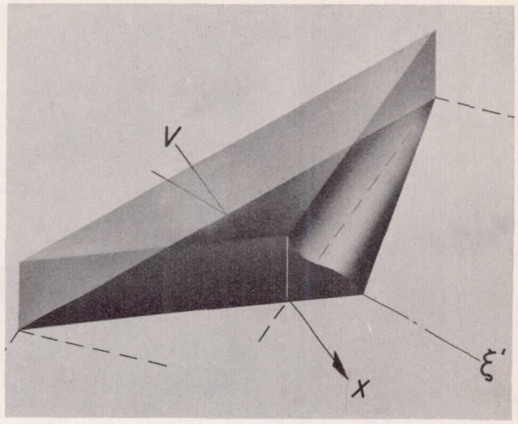
$$\left(\frac{\Delta P}{q}\right)_{E_3^*} = \frac{4\alpha(m^2+2mB-1)}{\sqrt{B^2(m^2+2mB-1)-(B+2m-m^2B)}}$$

---

[a]Left leading edge hits Mach cone from apex.

F.

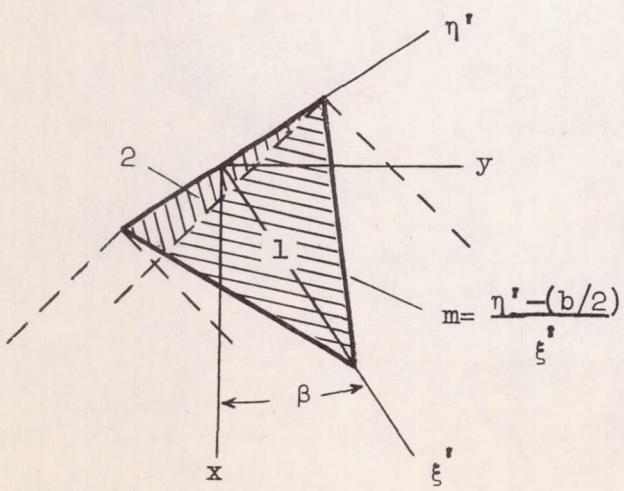


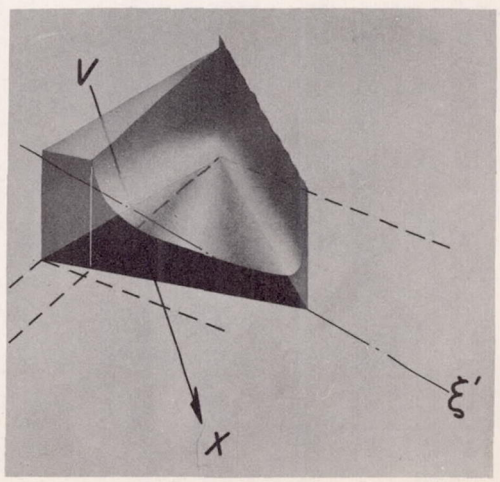


$$\left(\frac{\Delta P}{q}\right)_{F_1} = \frac{8\alpha}{\pi\sqrt{B^2-\tan^2\beta}} \tan^{-1}\sqrt{\frac{\left[m-\frac{\eta'-(b/2)}{\xi'}\right](B-\tan\beta)}{\left[\frac{\eta'-(b/2)}{\xi'}\right](B-\tan\beta)+(1+B\tan\beta)}}$$

$$\left(\frac{\Delta P}{q}\right)_{F_2} = \frac{4\alpha}{\sqrt{B^2-\tan^2\beta}}$$

G.





$$\left(\frac{\Delta P}{q}\right)_{G_1} = \frac{8\alpha}{\pi\sqrt{B^2-\tan^2\beta}}\left[\frac{(m+\tan\beta)(B-\tan\beta)}{B(m+\tan\beta)+(1-m\tan\beta)} \times \right.$$

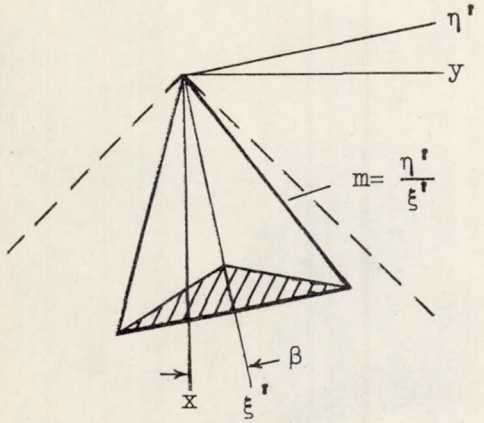
$$\sqrt{\frac{\left[\frac{\eta'-(b/2)}{\xi'}\right](B-\tan\beta)+(1-B\tan\beta)}{\left[m-\frac{\eta'-(b/2)}{\xi'}\right](B-\tan\beta)}} +$$

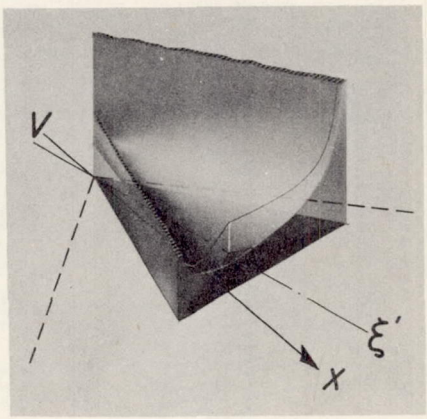
$$\left. \tan^{-1}\sqrt{\frac{\left[m-\frac{\eta'-(b/2)}{\xi'}\right](B-\tan\beta)}{\left[\frac{\eta'-(b/2)}{\xi'}\right](B-\tan\beta)+(1+B\tan\beta)}}\right]$$

$$\left(\frac{\Delta P}{q}\right)_{G_2} = \frac{4\alpha}{\sqrt{B^2-\tan^2\beta}}$$

2. Swept-back wing components:

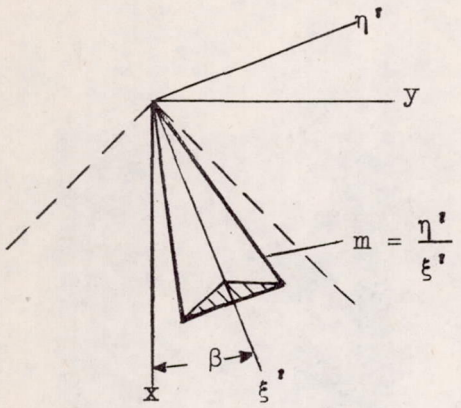
H.

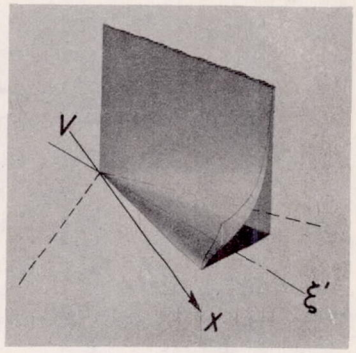




$$\left(\frac{\Delta P}{q}\right)_H = \left(\frac{\Delta P}{q}\right)_A$$

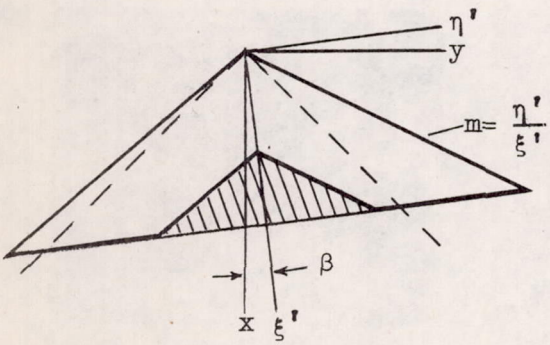
I.

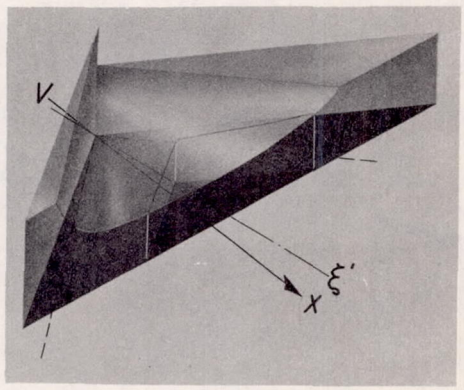




$$\left(\frac{\Delta P}{q}\right)_I = \left(\frac{\Delta P}{q}\right)_B$$

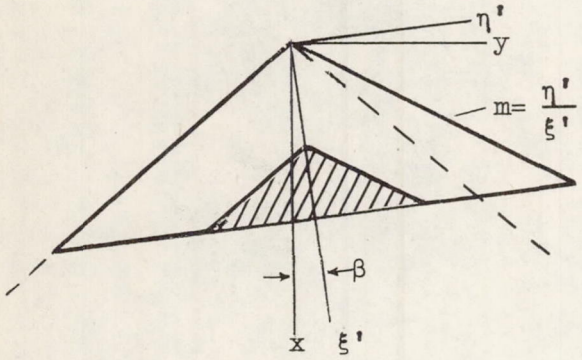
J. $\tan \beta < \frac{Bm-1}{B+m}$

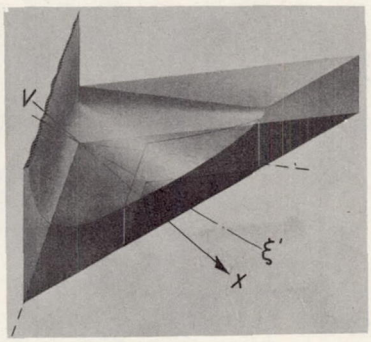




$$\left(\frac{\Delta P}{q}\right)_J = \left(\frac{\Delta P}{q}\right)_{E_2}$$

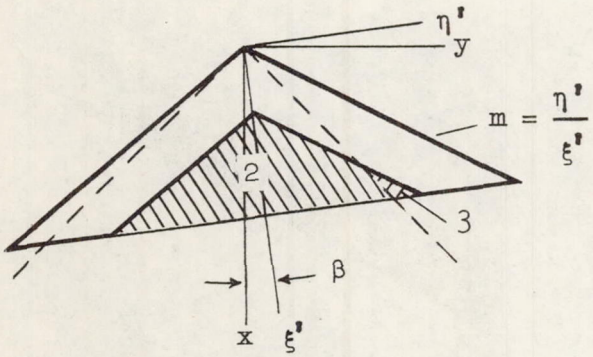
J*. $\tan \beta = \frac{Bm-1}{B+m}$ (See footnote b.)

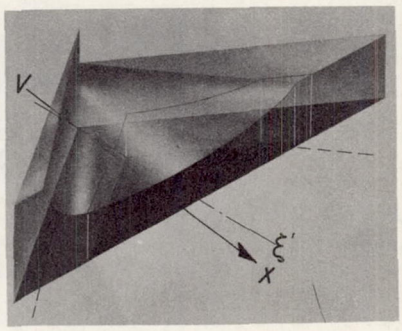




$$\left(\frac{\Delta P}{q}\right)_{J^*} = \left(\frac{\Delta P}{q}\right)_{E^*_2}$$

K. $\tan \beta < \frac{Bm-1}{B+m}$



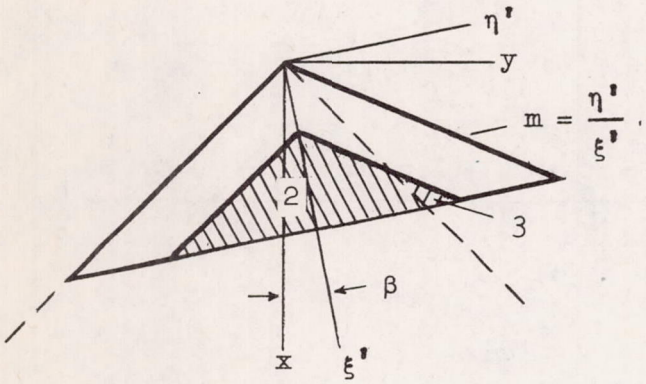


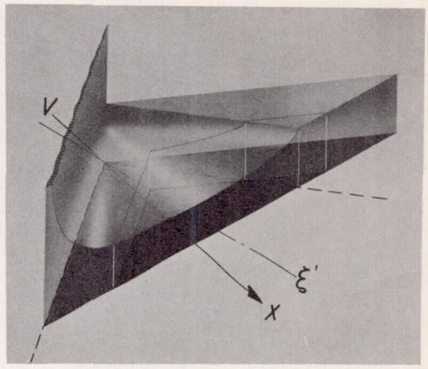
$$\left(\frac{\Delta P}{q}\right)_{K_2} = \left(\frac{\Delta P}{q}\right)_{E_2}$$

$$\left(\frac{\Delta P}{q}\right)_{K_3} = \left(\frac{\Delta P}{q}\right)_{E_3}$$

[b]Left leading edge hits Mach cone from apex.

$K^*. \tan \beta = \frac{Bm-1}{B+m}$ (See footnote b.)



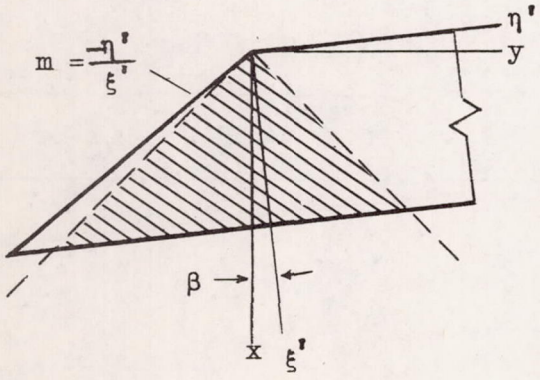


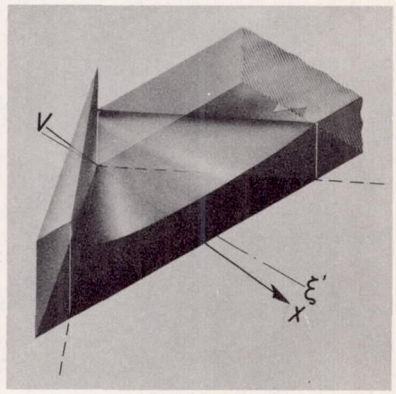
$$\left(\frac{\Delta P}{q}\right)_{K^*_2} = \left(\frac{\Delta P}{q}\right)_{E^*_2}$$

$$\left(\frac{\Delta P}{q}\right)_{K^*_3} = \left(\frac{\Delta P}{q}\right)_{E^*_3}$$

3. Trapezoidal wing components.

L.





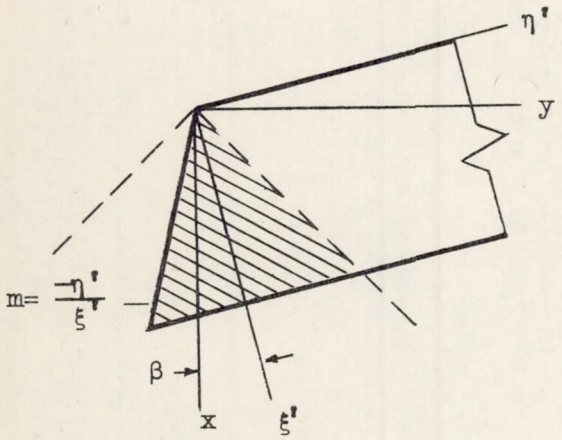
[b]Left leading edge hits Mach cone from apex

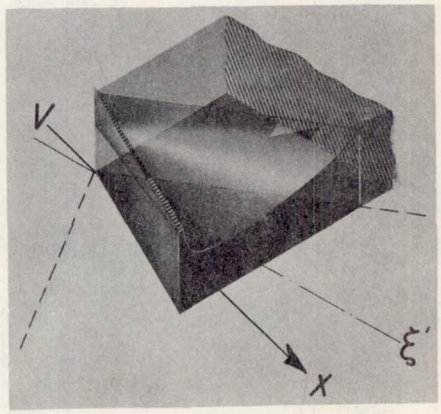
$$\left(\frac{\Delta P}{q}\right)_L = \frac{4\alpha}{\pi\sqrt{B^2-\tan^2\beta}}\left[\frac{\pi}{2} + \sin^{-1}\frac{B^2\left(\frac{\eta'}{\xi'}+\tan\beta\right)+\left(1-\frac{\eta'}{\xi'}\tan\beta\right)\tan\beta}{B(1+\tan^2\beta)}\right] +$$

$$\frac{4\alpha(m-\tan\beta)}{\pi\sqrt{B^2(m-\tan\beta)^2-(1+m\tan\beta)^2}}$$

$$\left[\frac{\pi}{2} - \sin^{-1}\frac{B^2(m-\tan\beta)\left(\frac{\eta'}{\xi'}+\tan\beta\right)+(1+m\tan\beta)\left(1-\frac{\eta'}{\xi'}\tan\beta\right)}{B\left(m+\frac{\eta'}{\xi'}\right)(1+\tan^2\beta)}\right]$$

M.

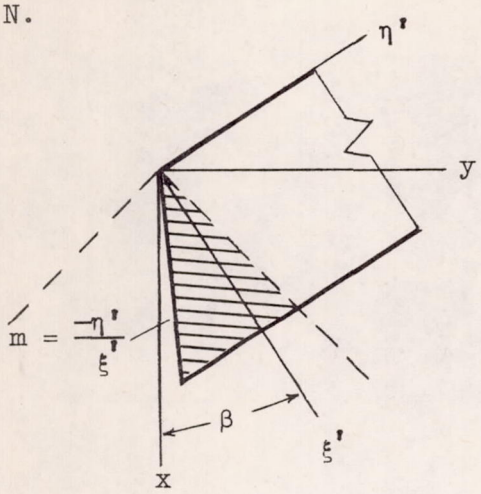


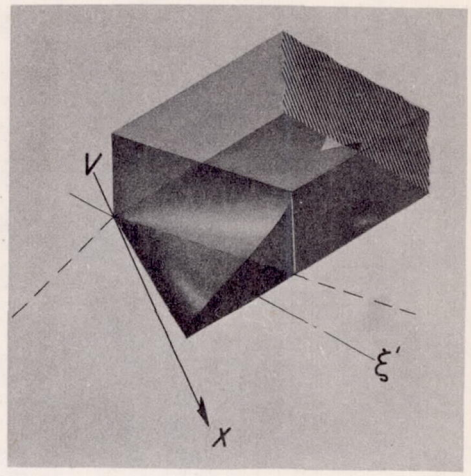


$$\left(\frac{\Delta P}{q}\right)_M = \frac{8\alpha}{\pi\sqrt{B^2-\tan^2\beta}}\left[\frac{(m-\tan\beta)(B+\tan\beta)}{B(m-\tan\beta)+(1+m\tan\beta)}\sqrt{\frac{(1-B\tan\beta)-\frac{\eta'}{\xi'}(B+\tan\beta)}{\left(m+\frac{\eta'}{\xi'}\right)(B+\tan\beta)}} +\right.$$

$$\left.\tan^{-1}\sqrt{\frac{\left(m+\frac{\eta'}{\xi'}\right)(B+\tan\beta)}{(1-B\tan\beta)-\frac{\eta'}{\xi'}(B+\tan\beta)}}\right]$$

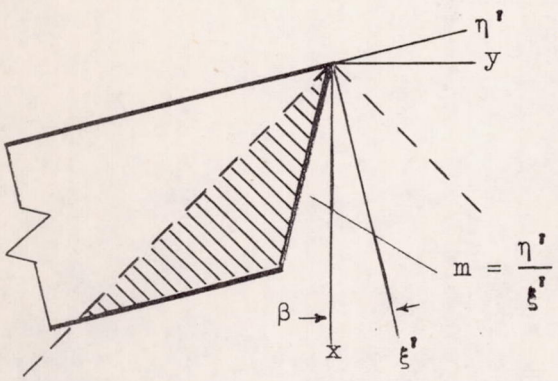
N.

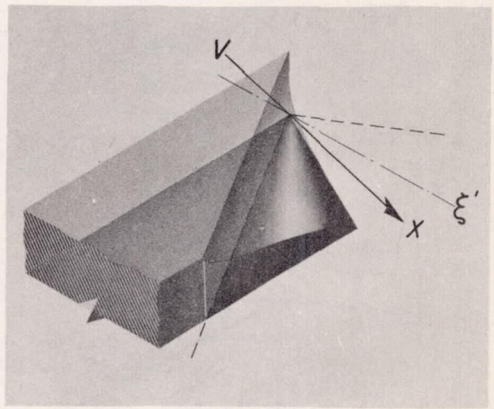




$$\left(\frac{\Delta P}{q}\right)_N = \frac{8\alpha}{\pi\sqrt{B^2-\tan^2\beta}} \tan^{-1}\sqrt{\frac{(m+\frac{\eta'}{\xi'})(B+\tan\beta)}{(1-B\tan\beta)-\frac{\eta'}{\xi'}(B+\tan\beta)}}$$

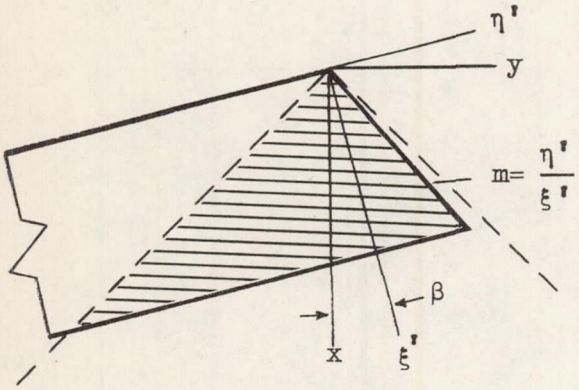
O.

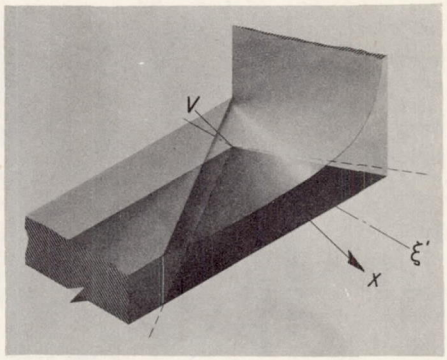




$$\left(\frac{\Delta P}{q}\right)_O = \frac{8\alpha}{\pi\sqrt{B^2-\tan^2\beta}} \tan^{-1}\sqrt{\frac{(m-\frac{\eta'}{\xi'})(B-\tan\beta)}{(1+B\tan\beta)+\frac{\eta'}{\xi'}(B-\tan\beta)}}$$

P.

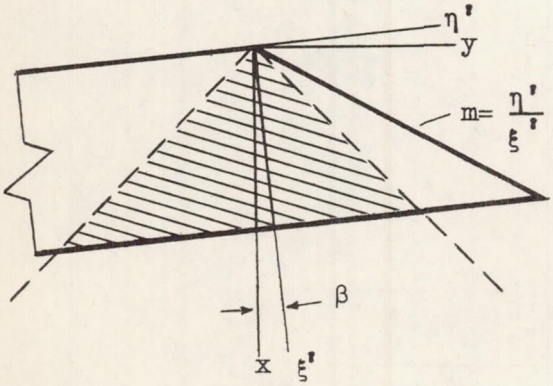


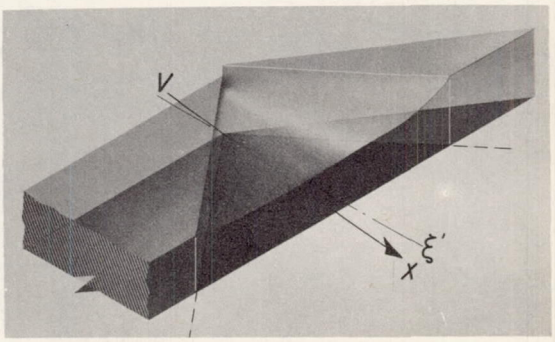


$$\left(\frac{\Delta P}{q}\right)_P = \frac{8\alpha}{\pi\sqrt{B^2-\tan^2\beta}}\left[\frac{(m+\tan\beta)(B-\tan\beta)}{B(m+\tan\beta)+(1-m\tan\beta)}\sqrt{\frac{(1+B\tan\beta)+\frac{\eta'}{\xi'}(B-\tan\beta)}{(m-\frac{\eta'}{\xi'})(B-\tan\beta)}}+\right.$$

$$\left.\tan^{-1}\sqrt{\frac{(m-\frac{\eta'}{\xi'})(B-\tan\beta)}{(1+B\tan\beta)+\frac{\eta'}{\xi'}(B-\tan\beta)}}\right]$$

Q.



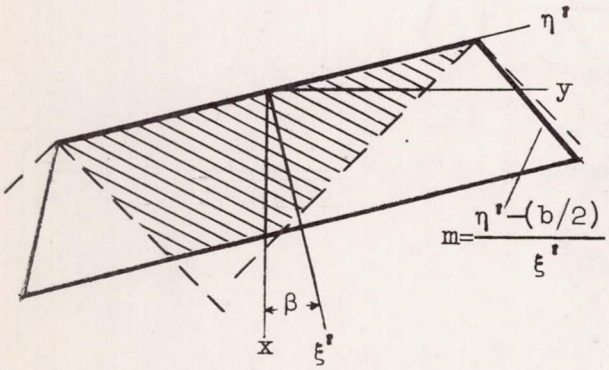


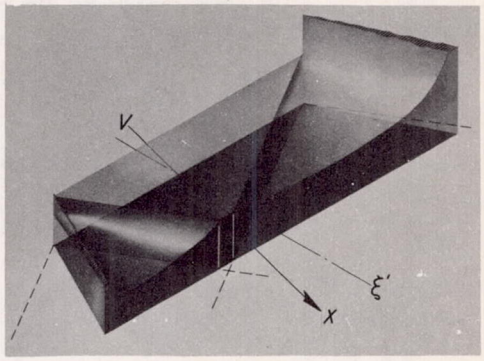
$$\left(\frac{\Delta P}{q}\right)_Q = \frac{4\alpha}{\pi\sqrt{B^2-\tan^2\beta}}\left[\frac{\pi}{2} - \sin^{-1}\frac{B^2\left(\frac{\eta'}{\xi'}+\tan\beta\right)+\left(1-\frac{\eta'}{\xi'}\tan\beta\right)\tan\beta}{B(1+\tan^2\beta)}\right] +$$

$$\frac{4\alpha(m+\tan\beta)}{\pi\sqrt{B^2(m+\tan\beta)^2-(1-m\tan\beta)^2}}$$

$$\left[\frac{\pi}{2} + \sin^{-1}\frac{B^2\left(\frac{\eta'}{\xi'}+\tan\beta\right)(m+\tan\beta)-(1-m\tan\beta)\left(1-\frac{\eta'}{\xi'}\tan\beta\right)}{B\left(m-\frac{\eta'}{\xi'}\right)(1+\tan^2\beta)}\right]$$

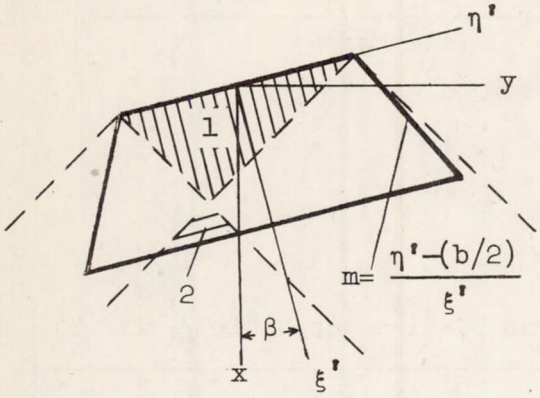
R.

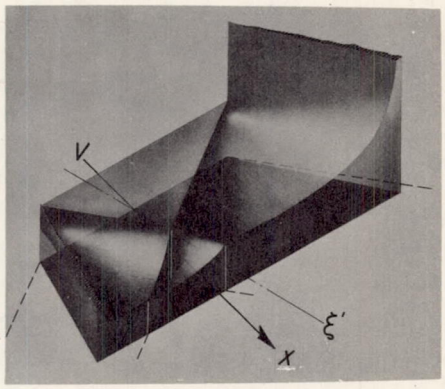




$$\left(\frac{\Delta P}{q}\right)_R = \frac{4\alpha}{\sqrt{B^2-\tan^2\beta}}$$

R*.





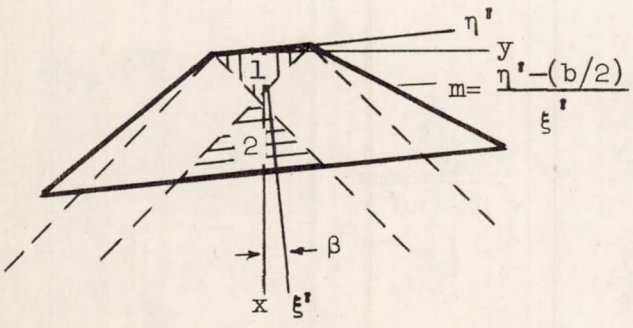
$$\left(\frac{\Delta P}{q}\right)_{R_1*} = \left(\frac{\Delta P}{q}\right)_R$$

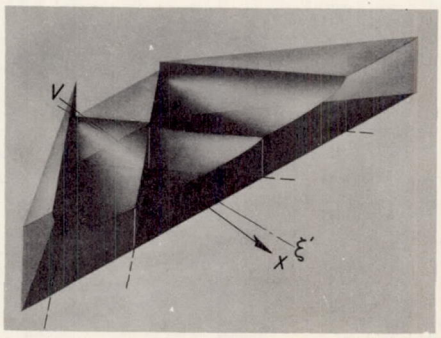
$$\left(\frac{\Delta P}{q}\right)_{R_2*} = \left(\frac{\Delta P}{q}\right)_M + \left(\frac{\Delta P}{q}\right)_P - \left(\frac{\Delta P}{q}\right)_R$$

where η' in $\left(\frac{\Delta P}{q}\right)_M$ should be replaced by $\eta' + \left(\frac{b}{2} - mc_r\right)$

η' in $\left(\frac{\Delta P}{q}\right)_P$ should be replaced by $\eta' - \left(\frac{b}{2} - mc_r\right)$

R**.





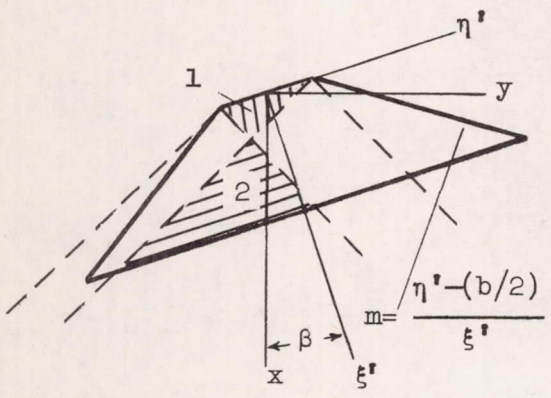
$$\left(\frac{\Delta P}{q}\right)_{R_1**} = \left(\frac{\Delta P}{q}\right)_R$$

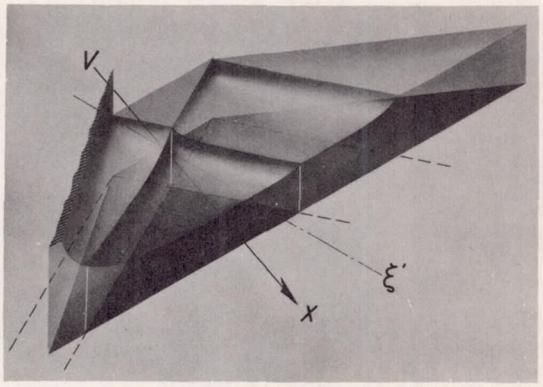
$$\left(\frac{\Delta P}{q}\right)_{R_2**} = \left(\frac{\Delta P}{q}\right)_L + \left(\frac{\Delta P}{q}\right)_Q - \left(\frac{\Delta P}{q}\right)_R$$

where η' in $\left(\frac{\Delta P}{q}\right)_L$ should be replaced by $\eta' + \left(\frac{b}{2} - mc_r\right)$

η' in $\left(\frac{\Delta P}{q}\right)_Q$ should be replaced by $\eta' - \left(\frac{b}{2} - mc_r\right)$

R^{***}.





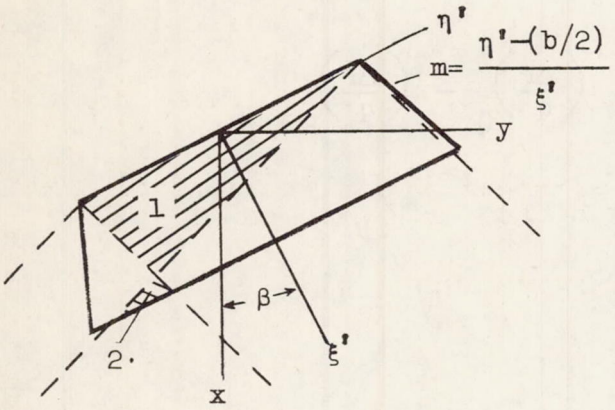
$$\left(\frac{\Delta P}{q}\right)_{R_1***} = \left(\frac{\Delta P}{q}\right)_R$$

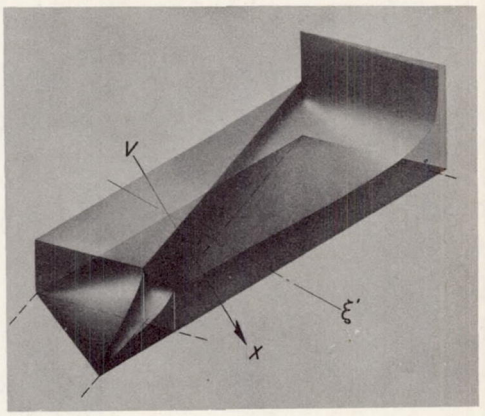
$$\left(\frac{\Delta P}{q}\right)_{R_2***} = \left(\frac{\Delta P}{q}\right)_M + \left(\frac{\Delta P}{q}\right)_Q - \left(\frac{\Delta P}{q}\right)_R$$

where η' in $\left(\frac{\Delta P}{q}\right)_M$ should be replaced by $\eta' + \left(\frac{b}{2} - mc_r\right)$

η' in $\left(\frac{\Delta P}{q}\right)_Q$ should be replaced by $\eta' - \left(\frac{b}{2} - mc_r\right)$

R****.





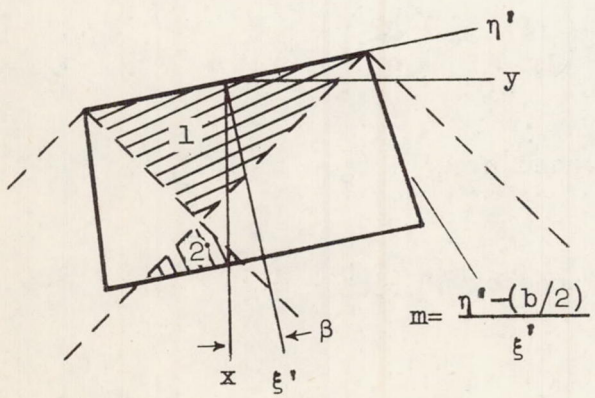
$$\left(\frac{\Delta P}{q}\right)_{R_1****} = \left(\frac{\Delta P}{q}\right)_R$$

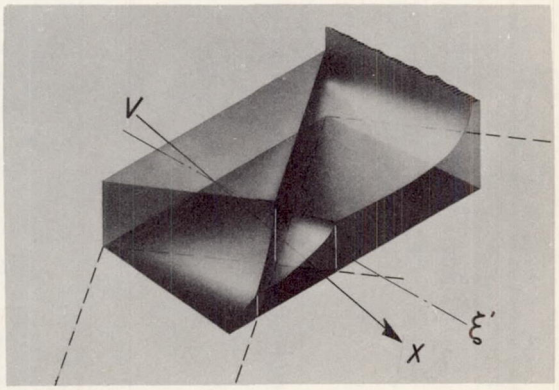
$$\left(\frac{\Delta P}{q}\right)_{R_2****} = \left(\frac{\Delta P}{q}\right)_N + \left(\frac{\Delta P}{q}\right)_Q - \left(\frac{\Delta P}{q}\right)_R$$

where η' in $\left(\frac{\Delta P}{q}\right)_N$ should be replaced by $\eta' + \left(\frac{b}{2} - mc_r\right)$

η' in $\left(\frac{\Delta P}{q}\right)_Q$ should be replaced by $\eta' - \left(\frac{b}{2} - mc_r\right)$

R*****.





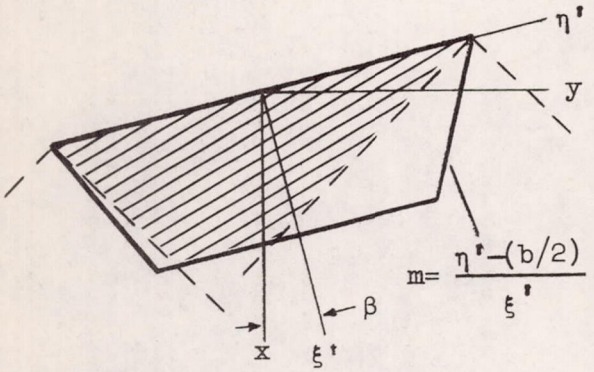
$$\left(\frac{\Delta P}{q}\right)_{R_1*****} = \left(\frac{\Delta P}{q}\right)_R$$

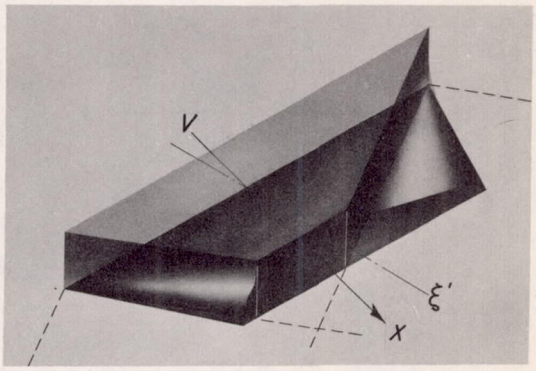
$$\left(\frac{\Delta P}{q}\right)_{R_2*****} = \left(\frac{\Delta P}{q}\right)_N + \left(\frac{\Delta P}{q}\right)_P - \left(\frac{\Delta P}{q}\right)_R$$

where η' in $\left(\frac{\Delta P}{q}\right)_N$ should be replaced by $\eta' + \left(\frac{b}{2} - mc_r\right)$

η' in $\left(\frac{\Delta P}{q}\right)_P$ should be replaced by $\eta' - \left(\frac{b}{2} - mc_r\right)$

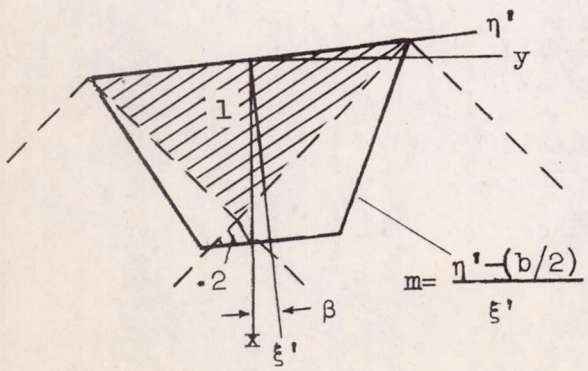
S.

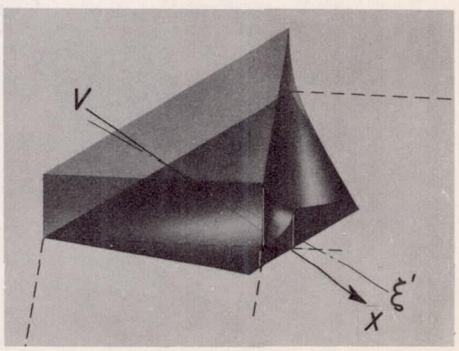




$$\left(\frac{\Delta P}{q}\right)_S = \frac{4\alpha}{\sqrt{B^2 - \tan^2\beta}}$$

S*.





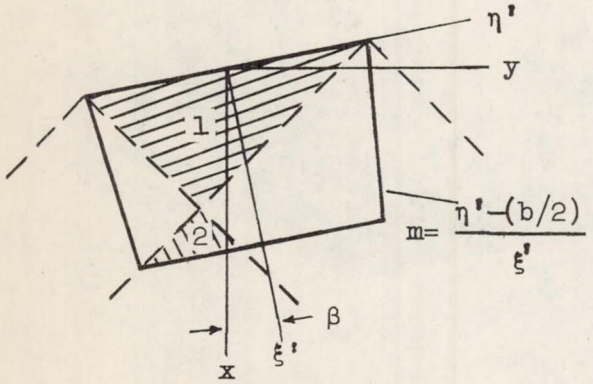
$$\left(\frac{\Delta P}{q}\right)_{S_1*} = \left(\frac{\Delta P}{q}\right)_S$$

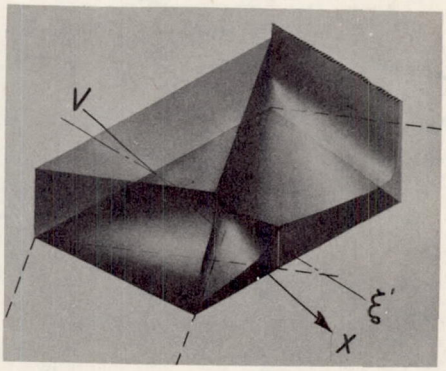
$$\left(\frac{\Delta P}{q}\right)_{S_2*} = \left(\frac{\Delta P}{q}\right)_N + \left(\frac{\Delta P}{q}\right)_O - \left(\frac{\Delta P}{q}\right)_{S'}$$

where η' in $\left(\frac{\Delta P}{q}\right)_N$ should be replaced by $\eta' + \frac{b}{2}$

η' in $\left(\frac{\Delta P}{q}\right)_O$ should be replaced by $\eta' - \frac{b}{2}$

S**.





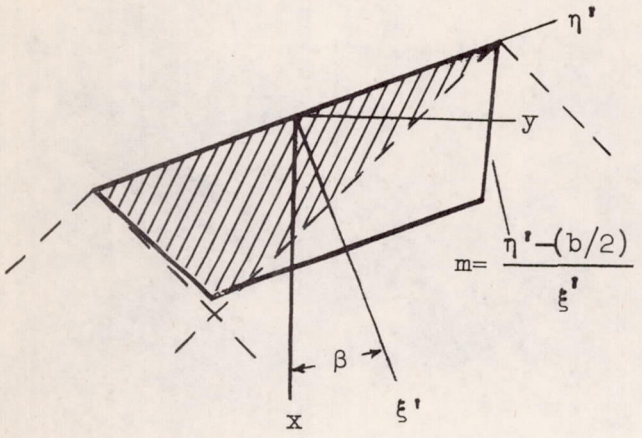
$$\left(\frac{\Delta P}{q}\right)_{S_1**} = \left(\frac{\Delta P}{q}\right)_S$$

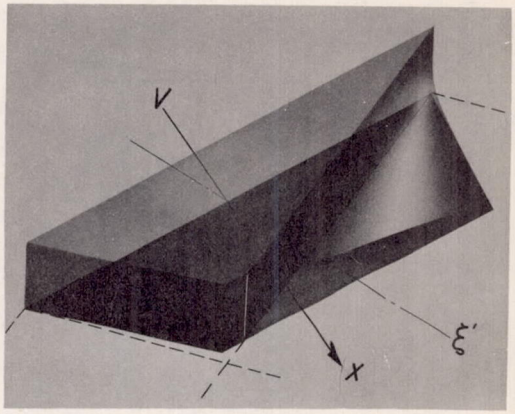
$$\left(\frac{\Delta P}{q}\right)_{S_2**} = \left(\frac{\Delta P}{q}\right)_N + \left(\frac{\Delta P}{q}\right)_P - \left(\frac{\Delta P}{q}\right)_S$$

where η' in $\left(\frac{\Delta P}{q}\right)_N$ should be replaced by $\eta' + \frac{b}{2}$

η' in $\left(\frac{\Delta P}{q}\right)_P$ should be replaced by $\eta' - \frac{b}{2}$

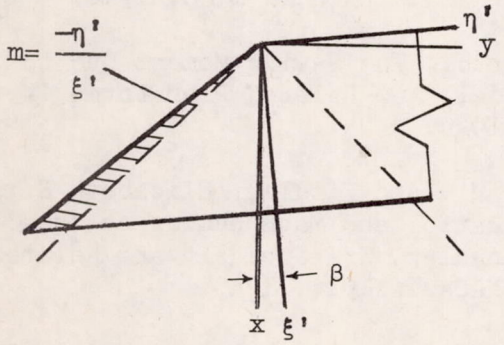
T.

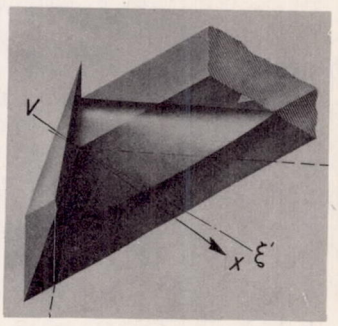




$$\left(\frac{\Delta P}{q}\right)_T = \frac{4\alpha}{\sqrt{B^2-\tan^2\beta}}$$

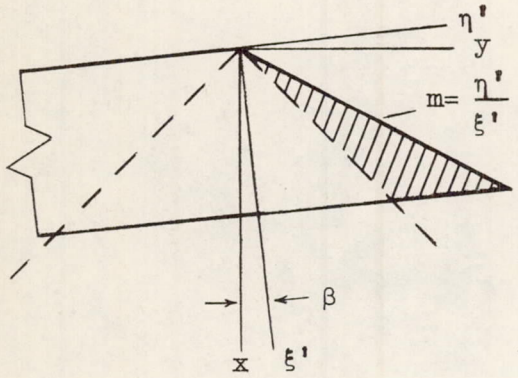
U.

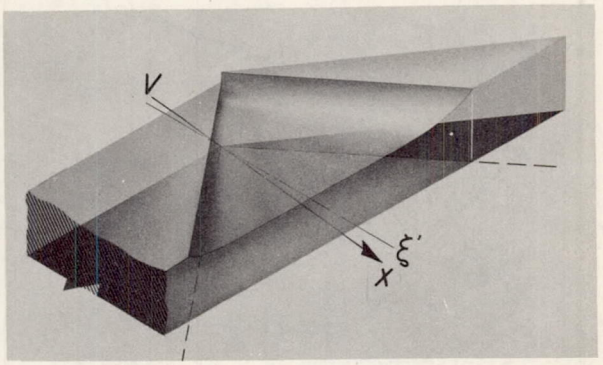




$$\left(\frac{\Delta P}{q}\right)_U = \frac{4\alpha(m-\tan\beta)}{\sqrt{B^2(m-\tan\beta)^2-(1+m\tan\beta)^2}}$$

V.





$$\left(\frac{\Delta P}{q}\right)_V = \frac{4\alpha(m+\tan\beta)}{\sqrt{B^2(m+\tan\beta)^2-(1-m\tan\beta)^2}}$$

REFERENCES

1. Jones, Arthur L., Spreiter, John R., and Alksne, Alberta: The Rolling Moment Due to Sideslip of Triangular, Trapezoidal, and Related Plan Forms in Supersonic Flow. NACA TN 1700, 1948.

2. Jones, Arthur L., and Alksne, Alberta: The Yawing Moment Due to Sideslip of Triangular, Trapezoidal, and Related Plan Forms in Supersonic Flow. NACA TN 1850, 1949.

3. Jones, Arthur L., Sorenson, Robert M., and Lindler, Elizabeth E.: The Effects of Sideslip, Aspect Ratio, and Mach Number on the Lift and Pitching Moment of Triangular, Trapezoidal, and Related Plan Forms in Supersonic Flow. NACA TN 1916, 1949.

4. Heaslet, Max. A., Lomax, Harvard, and Jones, Arthur L.: Volterra's Solution of the Wave Equation as Applied to Three-Dimensional Supersonic Airfoil Problems. NACA TN 1412, 1947.

5. Heaslet, Max. A., and Lomax, Harvard: The Use of Source-Sink and Doublet Distributions Extended to the Solution of Arbitrary Boundary Value Problems in Supersonic Flow. NACA TN 1515, 1948.

6. Evvard, John C.: Theoretical Distribution of Lift on Thin Wings at Supersonic Speeds (An Extension). NACA TN 1585, 1948.

7. Busemann, Adolph: Infinitesimal Conical Supersonic Flow. NACA TM 1100, 1947.

8. Lagerstrom, P. A.: Linearized Supersonic Theory of Conical Wings. NACA TN 1685, 1948.

9. Heaslet, Max. A., and Lomax, Harvard: The Application of Green's Theorem to the Solution of Boundary-Value Problems in Linearized Supersonic Wing Theory. NACA TN 1767, 1949.

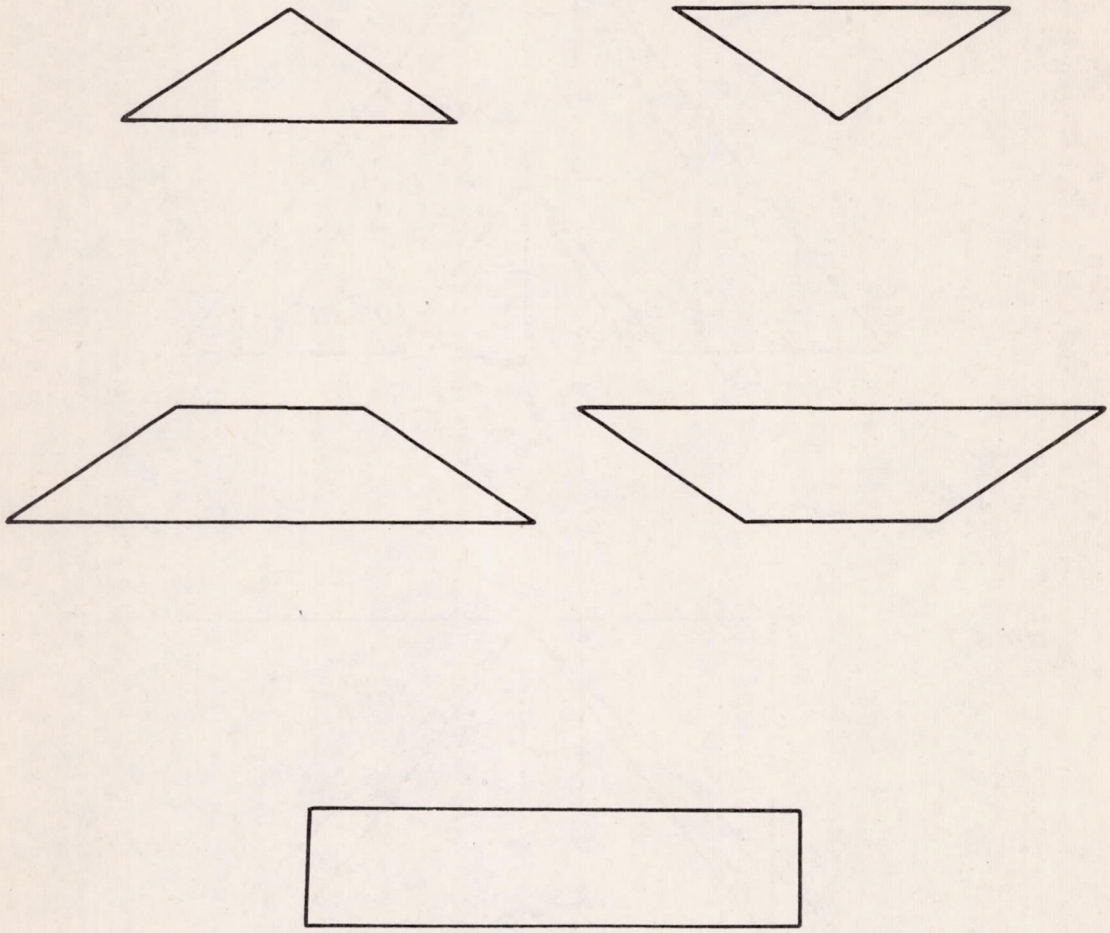


Figure 1.—The triangular, trapezoidal, and rectangular plan-form types investigated.

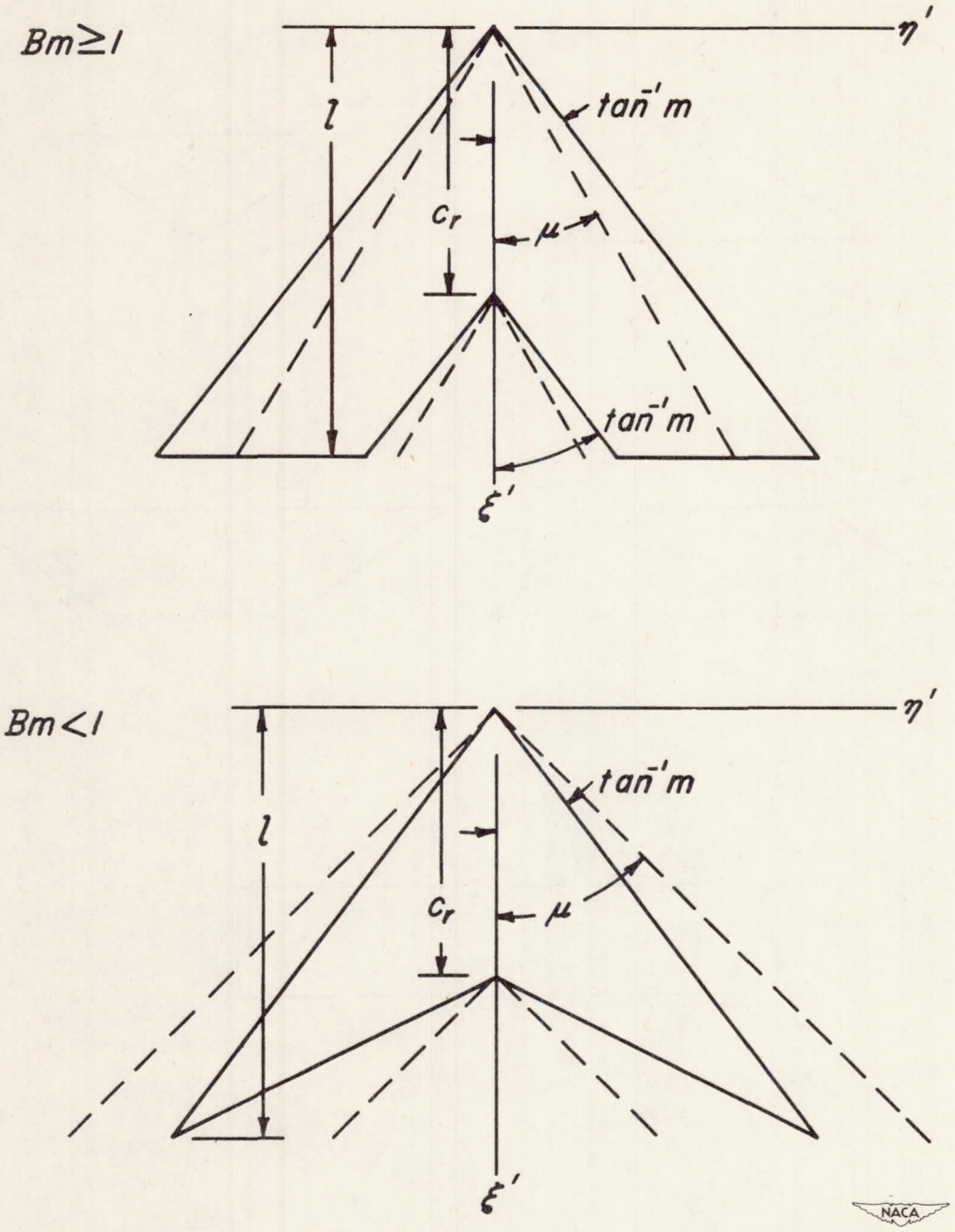
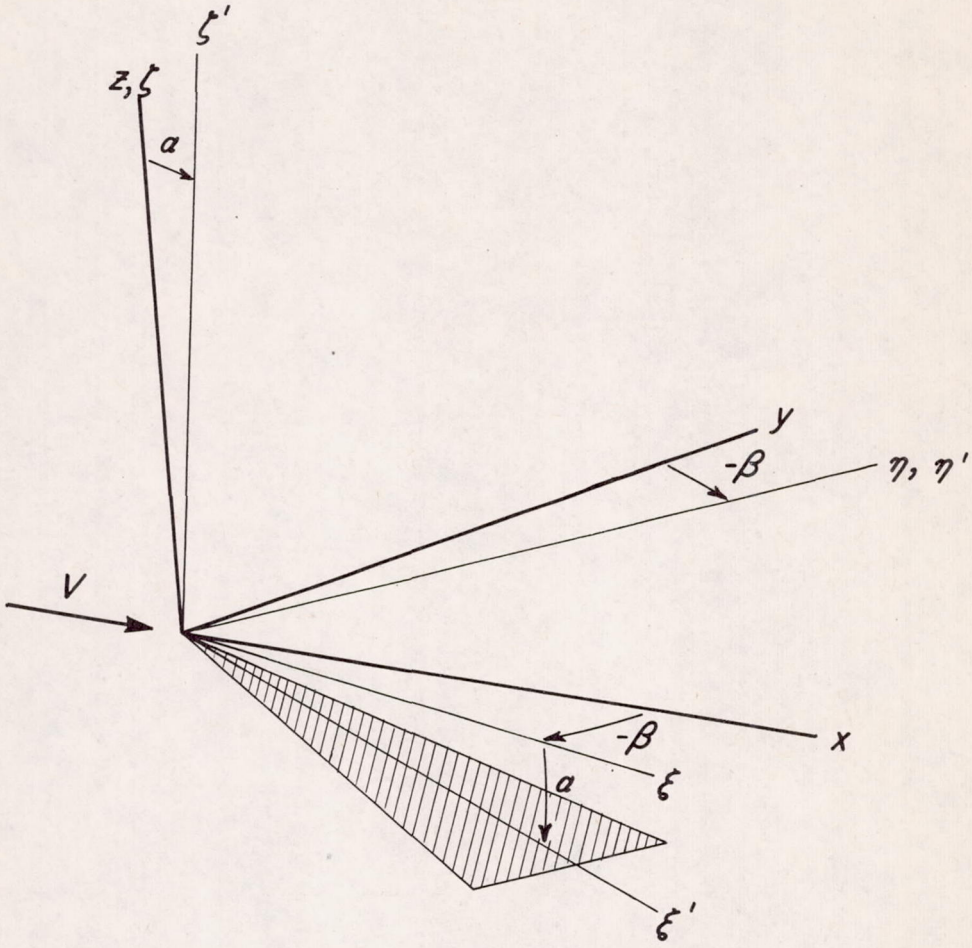


Figure 2.– Swept-back plan forms and Mach cone configurations investigated.



x, y, z rectangular coordinates of wind axes
ξ, η, ζ rectangular coordinates of stability axes
ξ', η', ζ' rectangular coordinates of body axes

Figure 3. – Coordinate axes systems used in analysis.